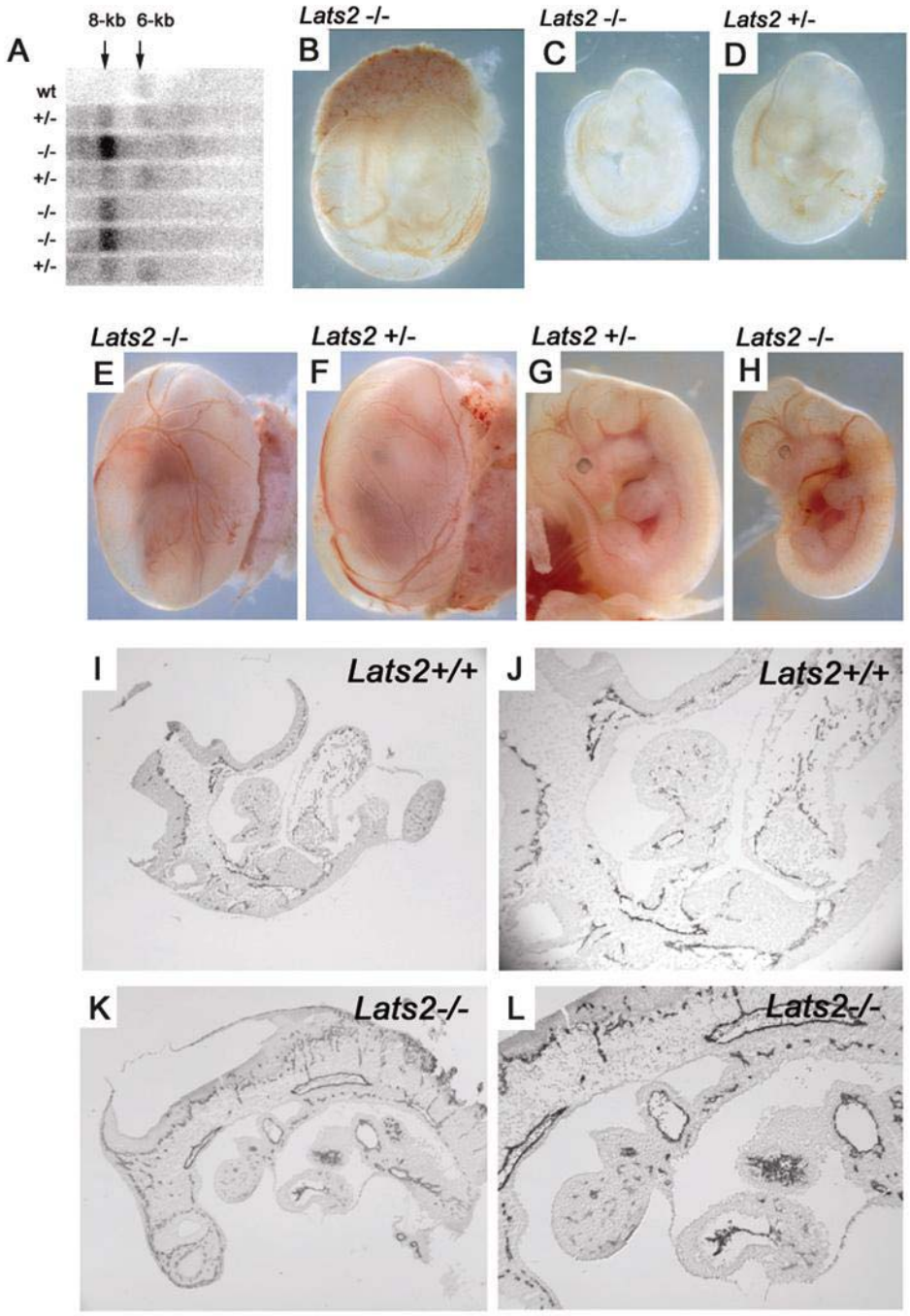

Supplementary Figure 1. **A**, Northern analysis of RNA extracted from E9.5 embryos derived from *Lats2*$^{+/-}$ heterozygous mating. RNA extracted from each embryo (5 μg) was denatured, separated on a formaldehyde-agarose gel, and transferred to a nylon membrane (Hybond-N^{+}, Amersham) according to standard methodology. The membrane was hybridized with a probe derived from a full-length *Lats2* cDNA probe. Embryos were genotyped using PCR from yolk sac gDNA. **B-H,** Representative photomicrographs depicting yolk sac morphology of *Lats2*$^{-/-}$ embryos. Whole mount photos of embryos at E9.5 (**B-D**) and E12.5 (**E-H**). *Lats2*$^{-/-}$ embryos from E9.5 to E12.5 exhibited normal

placental morphology, normal yolk sac morphology, normal yolk sac vascularization and blood islands. The *Lats2*$^{-/-}$ E9.5 embryo depicted (**B,C**) exhibited decreased BrdU incorporation (not shown) compared to the heterozygous control (**D**). **I-L,** Representative immunohistochemical detection of PECAM (CD31) in whole embryonic sections (**I,K**) and cardiac regions (**J,L**) from wild-type and *Lats2*$^{-/-}$ embryos.

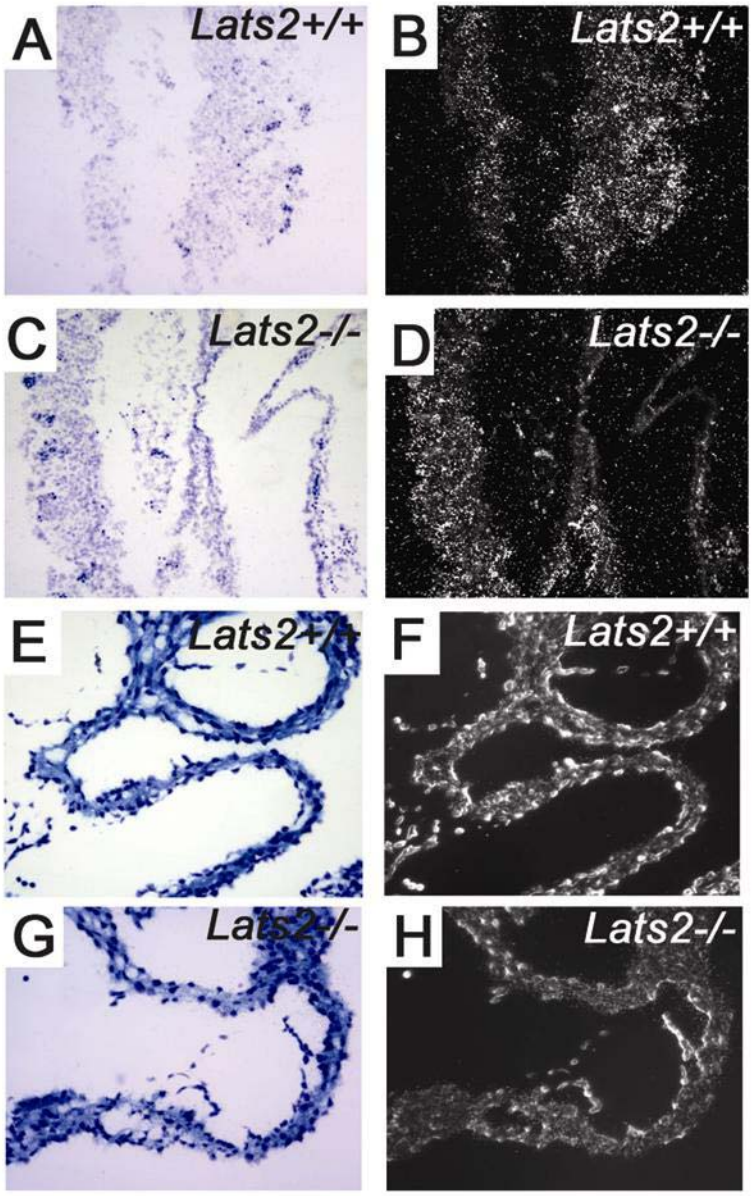

Supplementary Figure 2. A-D, PPARγ expression in placentae derived from wild-type and *Lats2*$^{-/-}$ E10.5 embryos as determined by *in situ* hybridization. **E-H**, Nkx2.5 expression in cardiac region of wild-type and *Lats2*$^{-/-}$ E9.5 embryos as determined by *in situ* hybridization.

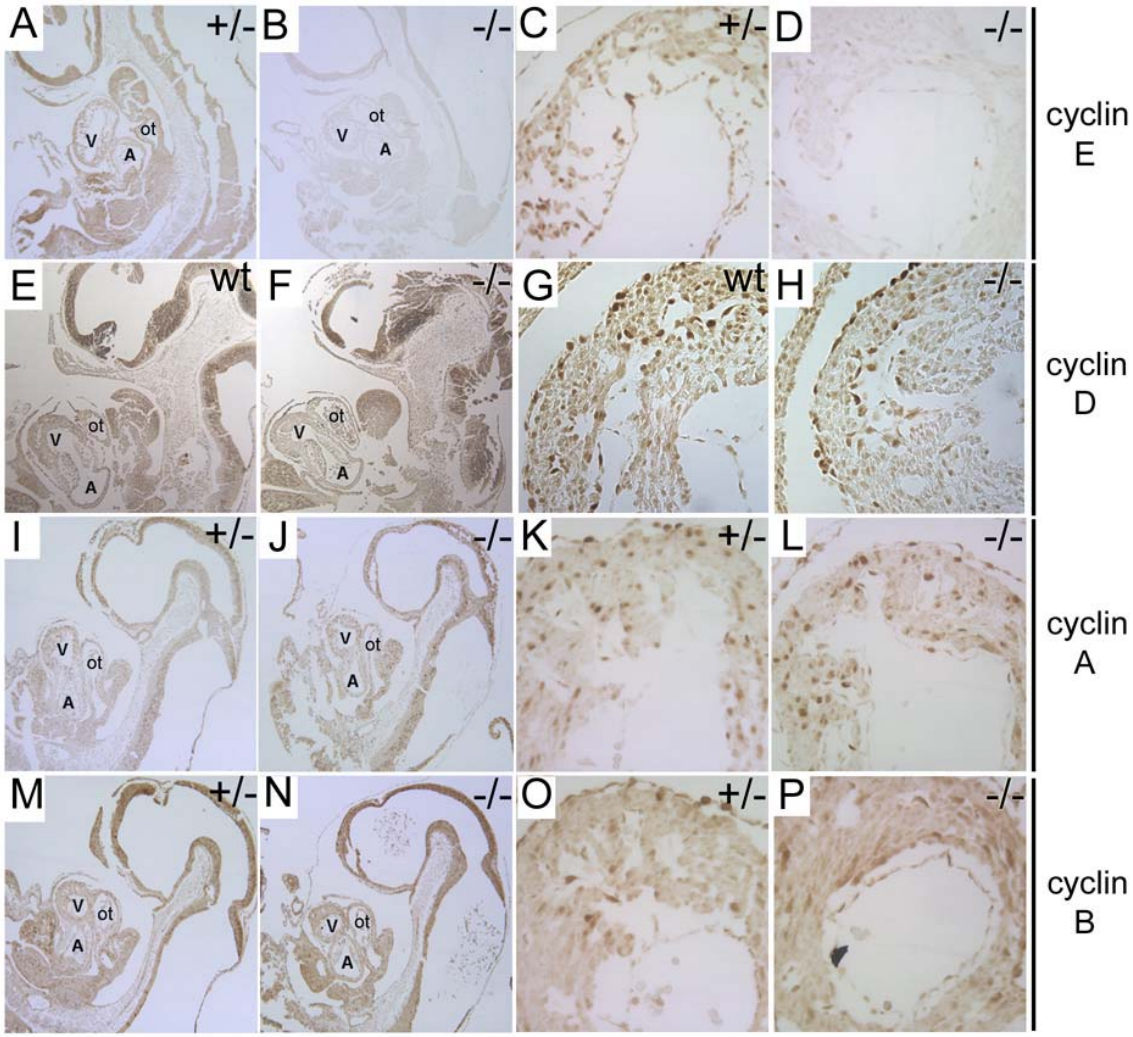

Supplementary Figure 3. Cyclin expression in Lats2-deficient E10.5 embryos. Immunostaining of E10.5 mid-sagital embryonic sections using antibodies specific for cyclin E **(A-D)**; cyclin D **(E-H)**; cyclin A **(I-L)** or cyclin B **(M-P)**. **A,B,E,F,I,J.M,N,** mid-sagital sections of E10.5 embryos at 5X magnification (v, ventricle; ot, outflow tract; A, atrium). **C,D,G,H,K,L,O,P,** heart ventricle at 40X magnification.

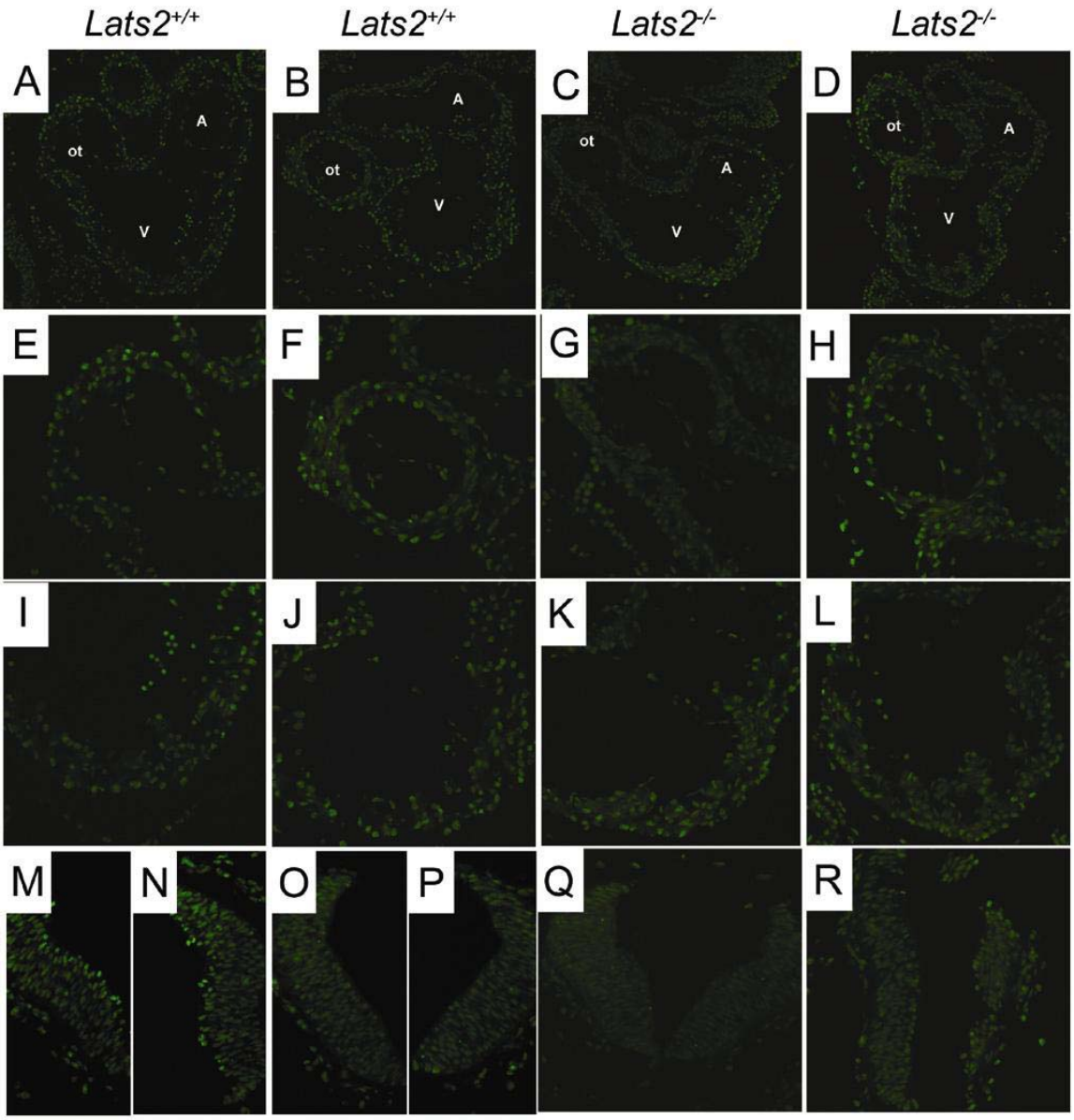

Supplementary Figure 4. TUNEL analysis for apoptosis of E9.5 embryos. Horizontal sections through the heart show no apoptotic nuclei after TUNEL reaction performed to label nicks in DNA caused by apoptotic degradation. **A-D**, heart area at 20x magnification (ot, outflow tract; V, left side of common ventricle chamber; A, common atrial chamber). **E-H**, aortic arch at 40x magnification. **I-L,** ventricle at 40x magnification. **M-R**, neural tube area at 40x magnification shows normal apoptosis profiles for wild-type and *Lats2*$^{-/-}$ embryos. Brightness and contrast of images have been adjusted to show some background auto fluorescence of unstained cells for orientation purposes.

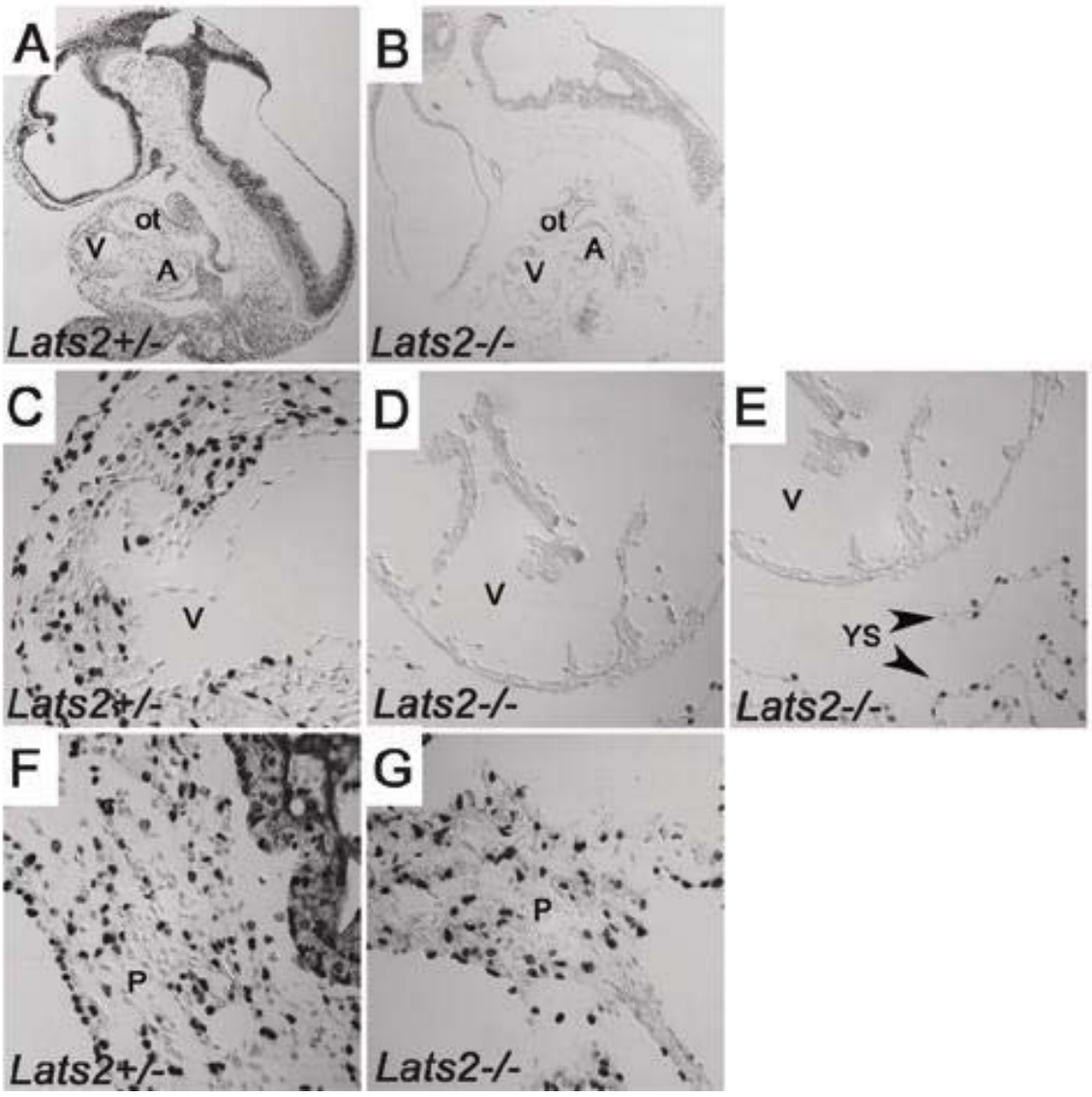

Supplementary Figure 5. A-G, BrdU incorporation in extraembryonic tissues of E10.5 *Lats2*$^{+/-}$ (**A,C,F**) and *Lats2*$^{-/-}$ (**B,D,E,G**) embryos (V, ventricle; ot, outflow tract; A, atrium; YS, yolk sac; P, placenta). The lack of BrdU incorporation in the *Lats2*$^{-/-}$ conceptus (**B,D,E,G**) contrasts with positively stained cells (arrowheads) seen in the extra-embryonic yolk sac (**E**) and placenta (**G**) that are comparable in number and staining intensity to the heterozygous littermate (**F**).

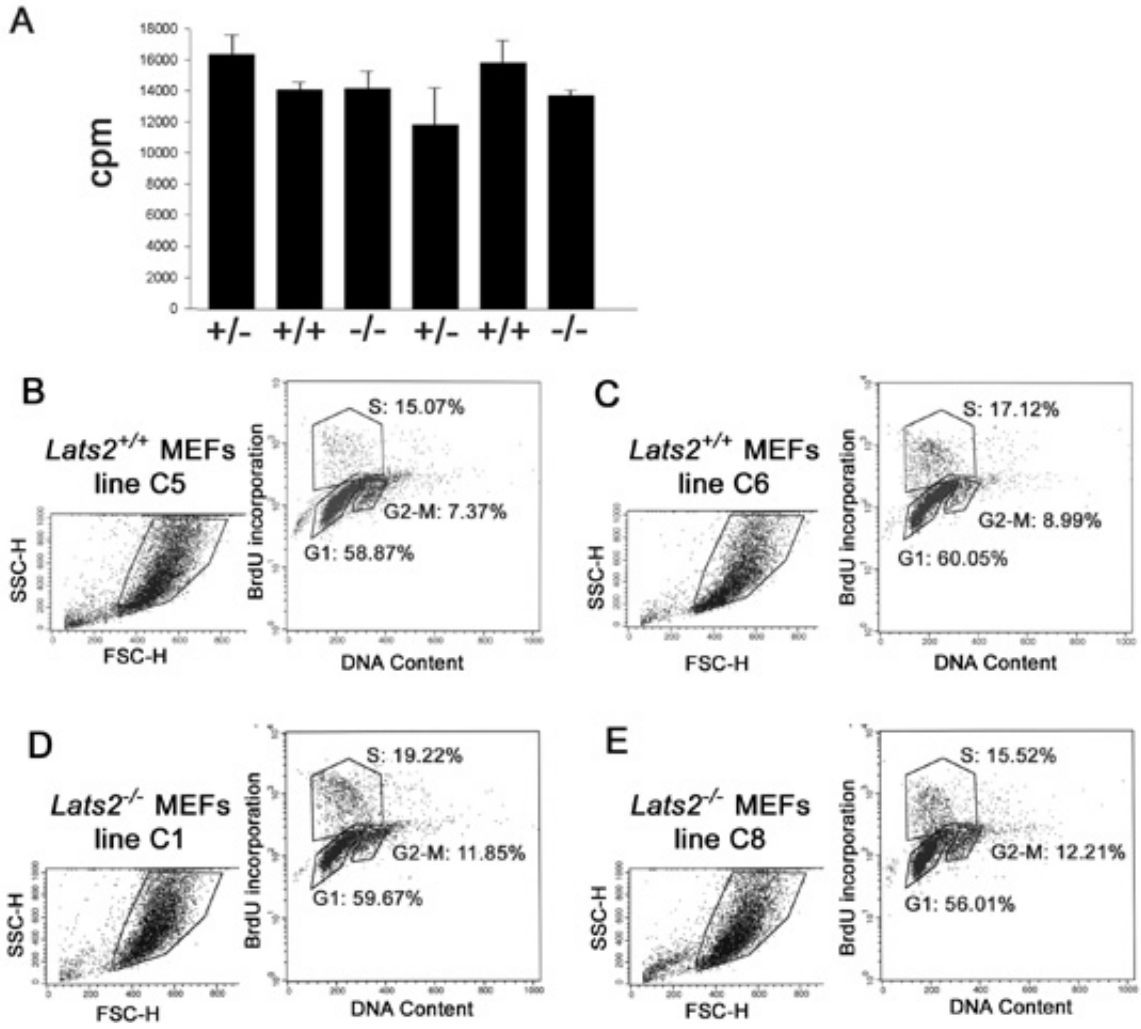

Supplementary Figure 6. A, No marked alteration in DNA synthesis was noted between wild-type and Lats2-deficient MEFS following examination of [^{3}H] Thymidine incorporation. **B-E**, No marked alteration in cell cycle parameters was observed in Lats2-deficient MEFs compared to wild-type MEFs, following BrdU incorporation/propidium iodide staining.

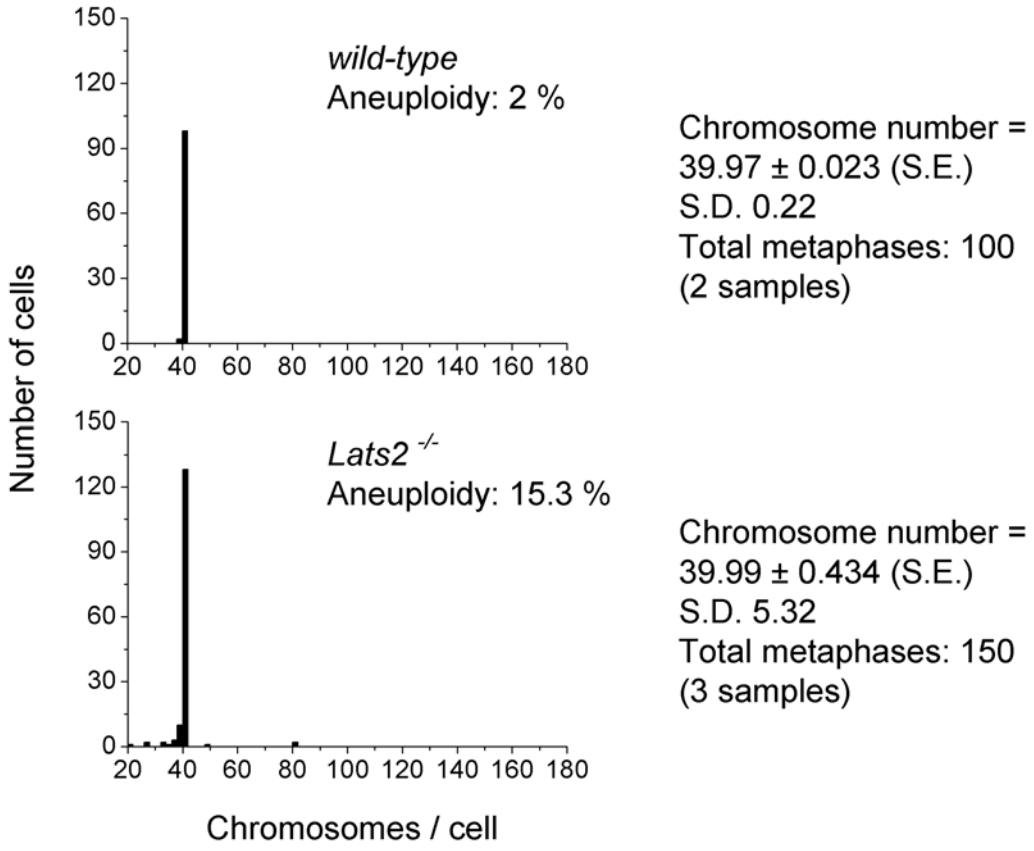

Supplementary Figure 7. Histograms depicting ploidy changes in wild-type and *Lats2*$^{-/-}$ embryos following colcemid treatment.